Color-tunable light emitting diodes based on quantum dot suspension

Zhenyue Luo, Haiwei Chen, Yifan Liu, Su Xu, and Shin-Tson Wu*

CREOL, The College of Optics and Photonics, University of Central Florida, Orlando, Florida 32816, USA

*Corresponding author: swu@ucf.edu

Received 30 December 2014; revised 19 February 2015; accepted 26 February 2015; posted 27 February 2015 (Doc. ID 231656); published 27 March 2015

We propose a color-tunable light emitting diode (LED) consisting of a blue LED as the light source and quantum dot (QD) suspension as the color-conversion medium. The LED color temperature can be controlled by varying the liquid volume of each QD suspension with different photoluminescence colors. We simulate and optimize the light efficiency and color quality of the color-tunable LED and also fabricated a prototype to prove concept. The proposed color-tunable LED exhibits several advantages such as excellent color-rendering property, simple structure and driving mechanism, as well as high energy efficiency. Its potential applications include circadian rhythm regulation and healthy lighting. © 2015 Optical Society of America

OCIS codes: (160.2540) Fluorescent and luminescent materials; (330.1715) Color, rendering and metamerism; (230.3670) Light-emitting diodes.

http://dx.doi.org/10.1364/AO.54.002845

1. Introduction

Light emitting diode (LED) technology has profoundly changed the way light is generated and has opened a wide field of applications [1]. In addition to energy saving and positive environmental effects, an LED light source is smart because its spatial, temporal, and color appearance can be designed to meet specific application requirements [2]. One typical and attractive lighting application is to use color temperature (CT) tunable white LED to dynamically vary the ambience of a room or office [3–6]. Environmental lighting has significant influence on the human body, including circadian rhythm, sleep behavior, cognition, alertness, and overall well-being [7–9]. For example, people tend to have higher working performance in high-CT lighting environments while relaxing well in low-CT lighting environments. An artificial light source, which replicates the sun's high CT during the daytime and low CT at night, could effectively regulate the human circadian rhythm (cycle of wake and sleep) and is beneficial to human productivity, well-being, and basic health.

Currently, CT tunable white LED is mainly realized by mixing LED clusters with different colors. Several LED cluster combinations have been discussed, including warm-white/cool-white cluster, red/green/blue cluster, and warm-white/green/blue cluster, etc. [3–6]. The CT of the output light can be fine-tuned through proper intensity control of each individual LED. Nevertheless, such a device has several demerits: It requires complicated and separate driving circuits for each LED, and it needs extra optical elements for proper color mixing of laterally placed light sources. Moreover, the CT cannot be tuned when all the LEDs are illuminating at maximum intensity. Instead of multi-chip LED clusters, a single-chip LED with color tunability is attractive since it is simple and stable.

Recently, quantum dot (QD) is emerging as a novel color-conversion medium [10]. QDs exhibit several attractive advantages over conventional phosphors: high quantum efficiency, broad absorption band, narrow emission linewidth, etc. More amazingly, its

1559-128X/15/102845-06$15.00/0

peak emission wavelength can be tuned by controlling the QD size or composition during chemical synthesis. Therefore, one can design the emission spectrum to get superb color-rendering properties and high light efficacy. QD has shown advantages in general lighting and liquid crystal display backlighting [7,11–16]. Recently, a QD lighting device with tunable color has been proposed and its feasibility analyzed numerically [17]. The authors purpose to use an electric field to tune the QD's luminescent properties such as absorption/emission cross-section and emission wavelength. However, such a device requires very high voltage (>100 V) to induce significant variation of material properties for spherical QD [18]. Nonspherical QD demands a lower voltage to change luminescent properties, but its quantum efficiency is much lower (<60%) compared to the spherical one [19]. Moreover, the device constantly requires a bias voltage to control the color and, thus, is power consuming.

In this paper we propose an alternative CT tunable white LED. The device consists of a blue LED as a pumping source and several QD suspensions as wavelength down-conversion modules. By changing the liquid volume of QD suspension, we can readily control the optical path length within the QD material and accordingly change the relative intensity of each color component. The device offers several advantages: (1) it uses blue LED, which has the highest quantum efficiency among visible LEDs, as a light source; (2) it has simple optics and electronics designs; (3) it possesses excellent color-rendering properties; (4) it can be driven by multiple mechanisms; and (5) it can be potentially multi-stable, which means an extra driving force is not needed when the emission CT is fixed. Therefore, the proposed CT tunable white LED could be attractive for smart environmental lighting applications.

2. Device Structure

Figure 1 shows the device structure of our proposed color-tuning white LED. The system consists of a blue (B) LED topped with a few color-conversion modules. Figure 1(a) shows a white LED with two color-conversion modules with red (R) and green (G) QDs. QDs absorb a portion of blue light and then re-emit R and G lights. A proper combination of RGB colors leads to white light with three emission peaks (tri-chromatic). Similarly, if the device consists of three wavelength down-conversion modules [Fig. 1(b)], then the output white light is quad-chromatic with four emission peaks.

Each color-conversion module contains two types of immiscible liquids: deionized water and QD suspension. The QD suspension was purchased from Cytodiagnostics. The QD materials (core-shell structure with CdS_xSe_{1-x} as core and ZnS as shell) were dissolved in toluene. The emitting color of the QDs can be controlled by changing the composition ratio x of the core material.

As Fig. 1 depicts, the chamber of the color-conversion module is made of acrylic glass and its top and bottom surfaces are sealed with transparent glass. The left sidewall has a flexible reservoir made of polymer membrane, while the right sidewall has a piston. This piston can be driven by multiple methods, e.g., step motor, magnetic method, or pneumatic effect [20–22].

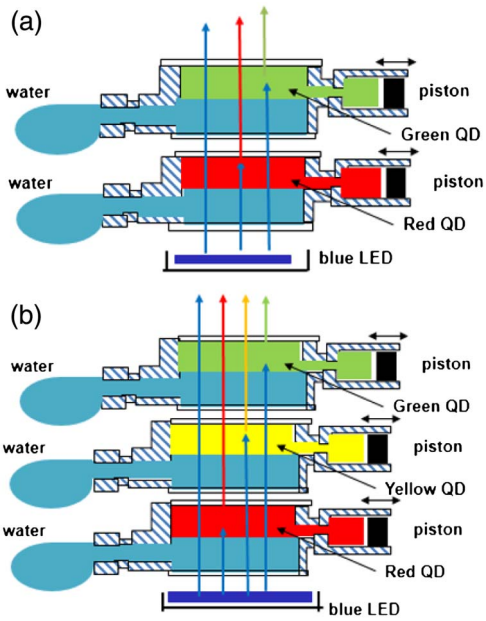

Fig. 1. Device structure of (a) tri-chromatic CT tunable white LED and (b) quad-chromatic CT tunable white LED.

As the piston moves, it either pushes or pulls the QD suspension; the liquid either fills into the flexible reservoir or flows back to the chamber. In this way, one can tune the volume ratio of QD suspension within the chamber and then control the light-path length in the QD suspension accordingly.

For the quad-chromatic CT tunable white LED shown in Fig. 1(b), the relative light intensity $f_i(i = r,y,g,b)$ of red, yellow, green, and blue can be written as

$$\begin{aligned} f_r &= A_r \times QY_r \times P_{b0}, \\ f_y &= (1-A_r) \times A_y \times QY_y \times P_{b0}, \\ f_g &= (1-A_r) \times (1-A_y) \times A_g \times QY_g \times P_{b0}, \\ f_b &= (1-A_r) \times (1-A_y) \times (1-A_g) \times P_{b0}. \end{aligned} \tag{1}$$

In Eq. (1) P_{b0} is the amount of blue light initially emitted from the blue LED, $QY_i(i = r,y,g)$ is quantum yield of each QD solution (here we assume $QY_i = 0.85$), and $A_i(i = r,y,g)$ is the absorption ratio of the blue light within each QD solution, which is given by

$$A_i = 1 - \exp(-\alpha_i d_i) \qquad (i = y,r,g). \tag{2}$$

In Eq. (2) d_i is the light-path length in each QD solution and α_i is the absorption coefficient of blue light in each QD solution. According to Eqs. (1) and (2),

each color component's relative intensity f_i can be controlled by changing the light-path length d_i in each QD suspension.

3. Spectrum Optimization for Color-Tunable LED

In this section we perform spectrum optimization for achieving high light efficacy and good color-rendering index (CRI). The spectral power distribution (SPD) of tri-chromatic and quad-chromatic white LEDs is expressed as

$$\begin{aligned} P_{\text{tri-chromatic}}(\lambda) &= f_b S(\lambda,\lambda_b,\Delta\lambda_b) + f_g S(\lambda,\lambda_g,\Delta\lambda_g) \\ &\quad + f_r S(\lambda,\lambda_r,\Delta\lambda_r), \\ P_{\text{quad-chromatic}}(\lambda) &= f_b S(\lambda,\lambda_b,\Delta\lambda_b) + f_g S(\lambda,\lambda_g,\Delta\lambda_g) \\ &\quad + f_y S(\lambda,\lambda_y,\Delta\lambda_y) + f_r S(\lambda,\lambda_r,\Delta\lambda_r). \end{aligned} \quad (3)$$

In Eq. (3) $S(\lambda,\lambda_b,\Delta\lambda_b)$ represents the blue LED emission spectrum transmitting through the color-conversion modules $S(\lambda,\lambda_g,\Delta\lambda_g)$, $S(\lambda,\lambda_y,\Delta\lambda_y)$, and $S(\lambda,\lambda_r,\Delta\lambda_r)$ are the emission spectra of green, yellow, and red QDs. Each emission spectra can be modeled as a Gaussian function with $\lambda_i (i = r,y,g,b)$ standing for the central wavelength, $\Delta\lambda_i$ for the full width half-maximum (FWHM), and f_i for the relative intensity.

Here we use the luminous efficacy of radiation (LER) [17] as a measure of light spectral efficiency, which is defined as

$$\text{LER} = \frac{683\frac{\text{lm}}{W_{\text{opt}}}\int P(\lambda)V(\lambda)\text{d}\lambda}{\int P(\lambda)\text{d}\lambda}. \quad (4)$$

LER reflects how efficiently the output light can be converted to the brightness perception of human eye. $V(\lambda)$ is the photopic eye sensitivity function centered at $\lambda = 550$ nm [12]. The maximum value of LER is 683 lm/W_{opt} for a monochromatic light source at $\lambda = 550$ nm. However, for a broadband light source (e.g., white light) its LER is usually much lower.

We also use CRI to quantitatively evaluate the color-rendering property of white light [1],

$$\text{CRI} = \frac{1}{8}\sum_{j=1}^{8} R_i \quad \text{where } R_j = 100 - 4.6\Delta E_j. \quad (5)$$

Here ΔE_j is the difference in color appearance for each of the eight reflective samples ($j = 1-8$) illuminated by the test and the reference light sources in the CIE 1964 color space.

In order to optimize the spectrum of the CT tunable LED, we introduce the following objective function for the tri-chromatic LED:

$$\begin{aligned} F_1(\lambda_b,\lambda_g,\lambda_r) &= \frac{1}{8}\sum_{i=1}^{8}\text{LER}_i, \\ F_2(\lambda_b,\lambda_g,\lambda_r) &= \frac{1}{8}\sum_{i=1}^{8}\text{CRI}_i. \end{aligned} \quad (6)$$

Here i ($i = 1-8$) refers to color temperature at 2700, 3000, 3500, 4000, 4500, 5000, 5700, and 6500 K, respectively. The objective function aims to optimize the averaged photometric and colorimetric properties at eight typical color temperatures.

For each emitted color, its central wavelength λ_i, FWHM $\Delta\lambda_i$, and relative intensity f_i can be used as variables to model the emission spectrum. In order to accelerate the optimization process, here we only used the central wavelengths as variables. From our simulations we found the optimization result is not sensitive to the FWHM values. Currently, the FWHM of a blue LED is 18–20 nm. Cadmium-based QD phosphor has FWHM around 30–40 nm, depending on the particle size distribution [11,12]. Thus, in our optimization process we fixed the FWHM as $\Delta\lambda_b = 20$ nm, $\Delta\lambda_g = 40$ nm, and $\Delta\lambda_r = 30$ nm for the tri-chromatic case. For tri-chromatic LED, once the color temperature is determined we can solve the color mixing function to obtain the relative intensity of each color component.

Similarly, we can rewrite Eq. (6) with $(\lambda_b,\lambda_g,\lambda_y,\lambda_r)$ as variables for quad-chromatic LED. In this case we also fix the FWHM of each emission peak as $\Delta\lambda_b = 20$ nm, $\Delta\lambda_g = \Delta\lambda_y = \Delta\lambda_r = 30$ nm.

An ideal light source should have both large LER and high CRI. It has been proven that these two objectives are mutually exclusive [17]. Instead of an optimal result that simultaneously satisfies both objectives, we should obtain a group of solutions within those. Further improvement of one objective must be compromised by the degradation of another objective. Such solutions constitute a so-called Pareto front. In this paper, we choose the particle swarm optimization algorithm as optimization solver to find the Pareto front [14].

We performed multi-objective optimization for tri-chromatic LED and quad-chromatic LED, respectively, and plot the optimization results in Fig. 2. The blue solid curve in Fig. 2(a) is the Pareto front of tri-chromatic white LED with color temperature fixed at 4000 K, while the black dashed curve shows the Pareto front of tri-chromatic color-tuning LED with LED and CRI averaged over eight color temperatures. The CT tunable LED could vary from relatively high CRI (~88) but limited LER (365 lm/w) to low CRI (<70) but high LER (>400 lm/w). The trade-off between LER and CRI is obvious because of the gain of one metric accompanied by the loss of the other. In general, the performance of color-tunable LED is slightly inferior to that of the LED fixed at 4000 K. This is reasonable because the CT tunable LED needs to balance the CRI and LER for all the color temperatures.

Figure 2(b) shows the Pareto front of a quad-chromatic optimized for LED with 4000 K (blue solid curve) as well as color-tunable LED (black dashed curve). Compared to the tri-chromatic case, the quad-chromatic LED manifests superior color-rendering property. In particular, the CT tunable quad-chromatic LED can have CRI over 95 while still

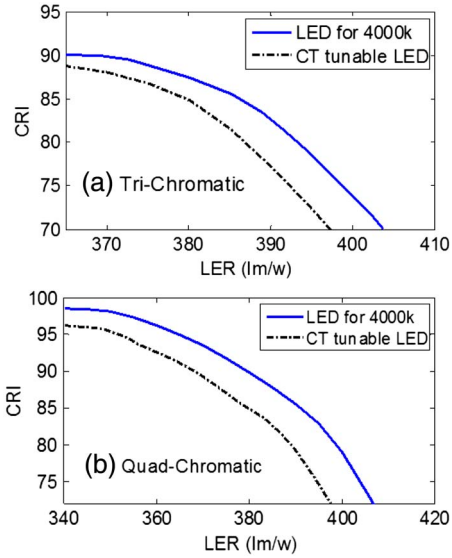

Fig. 2. Relationship between LER and CRI for white LED with (a) tri-chromatic and (b) quad-chromatic configurations. The black dashed curve represents the Pareto front for CT tunable white LED while the blue solid line represents the Pareto front white LED optimized for CT = 4000 K.

maintaining a reasonably high LER (>340 lm/w). It outperforms previously published color-tuning LEDs in obtaining high CRI and LER simultaneously [4,5].

Figure 3(a) shows an example of optimized tri-chromatic CT tunable white LED located on the Pareto front line. The emission peaks are located at $\lambda_b = 464.1$ nm, $\lambda_g = 544.0$ nm, and $\lambda_r = 614.2$ nm, respectively. Figure 3(a) shows the LED spectrum under four typical color temperatures (2700, 4000, 5000, and 6500 K). Only the intensity ratio varies while the central wavelength and the FHWM of each color component are fixed. White light is more reddish at low CT while it is bluish at high CT. Accordingly, the power ratio of the three-color components changes with CT. From low to high CT, the blue component gets stronger while the red component becomes weaker.

Figure 3(b) shows the LER and CRI at different CTs. Overall the averaged LER = 363.2 lm/W and averaged CRI = 88.3. As CT increases, the light source becomes more bluish, and accordingly the LER decreases since the human eye is less sensitive to blue color. The tri-chromatic LED has limited color-reproduction capability. To obtain higher CRI, we should use quad-chromatic LED.

To better evaluate the color-reproduction ability, we also calculated the color-quality scale (CQS) as suggested by the National Institute of Standards and Technology [23]. CQS is considered as a more objective measure of color-reproduction ability for color-saturated light sources. Our color-tuning LED shows an average CQS of 81.5.

Figure 4(a) shows the optimized spectrum for a quad-chromatic LED. The emission peaks are located at $\lambda_b = 458.9$ nm, $\lambda_g = 523.2$ nm, $\lambda_y = 570.0$ nm, and $\lambda_r = 619.3$ nm, respectively. The emitting light covers a broader spectral range and therefore it has better color-reproduction ability. Figure 4(b) depicts the LER and CRI at different CTs. On average, the LER is 347.2 lm/W and CRI is 95.8. Moreover, the average CQS value is greatly improved to 92.0. Therefore, increasing the color-conversion module is beneficial to enhance the color-rendering property.

To quantitatively evaluate the circadian effect, we also calculated the circadian action factor (CAF) of the proposed color-tunable LED. CAF is a measure of biological action per unit of visual response. Different CAF values are advisable depending on the time

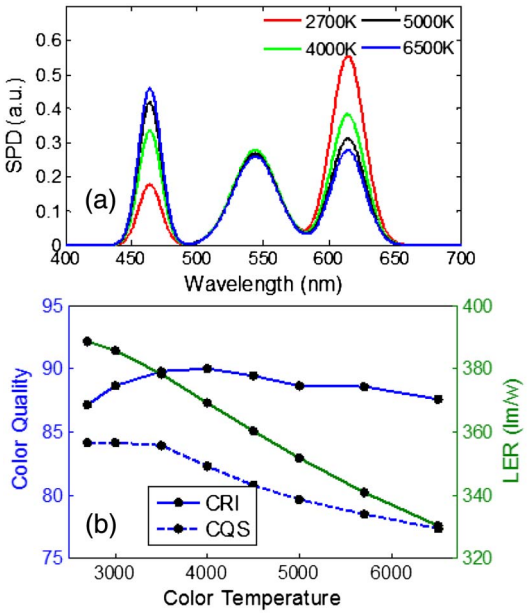

Fig. 3. (a) SPD of a tri-chromatic CT tunable white LED under different CT and (b) CRI, CQS, and LER of tri-chromatic CT tunable LED.

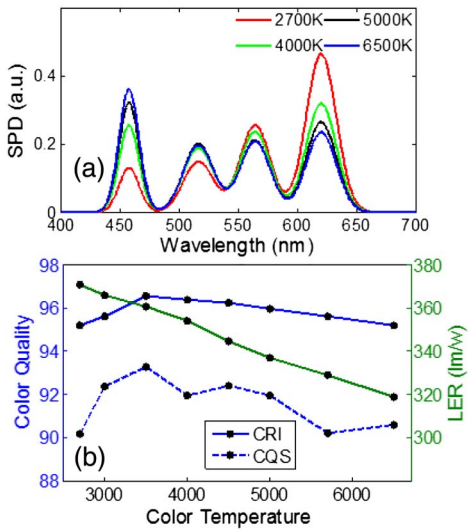

Fig. 4. (a) SPD of a quad-chromatic CT tunable white LED under different CTs and (b) CRI, CQS, and LER of quad-chromatic CT tunable LED.

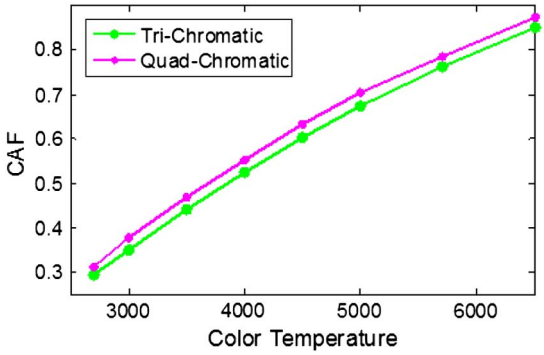

Fig. 5. Simulated CAF as a function of LED color temperature.

of day: high CAF during daytime and low CAF at night [8]. Figure 5 shows the CAF value of tri-chromatic and quad-chromatic color-tunable LEDs at different color temperatures. CAF increases as the color temperature rises. Therefore, we can tune the white LED at low CT during daytime to enhance working efficiency while setting a high CT during nighttime to improve sleep quality. In this way, the proposed color-tunable LED can be beneficial to human health and productivity.

4. Proof-of-Concept Experiment

To prove the concept we fabricated a prototype color-tuning LED, as shown in Fig. 6(a). The LED consists of one blue LED and one color-conversion module with a yellow QD whose diameter is around 2 cm. The weight percentage of QD in this suspension was 0.5%. We used a commercial syringe to act as a pump and drove it by an electric step motor (Newport ESP 300). Its step resolution is as fine as 2.5 μm. The electric step motor controls the piston position, which in turn tunes the yellow QD suspension thickness.

The emission spectrum of LED is recorded by an Ocean Optics USB2000 spectrometer. Figure 6(b) shows the recorded emission spectra when the QD suspension has a different thickness d. As the QD thickness increases, more blue light is absorbed and converted to yellow light. Figure 6(c) shows the color coordinates and the insets show the color image of the LED. With increased QD thickness, the emitted color varies from blue to white and finally to yellow.

To prove the concept, in our experiment we chose a simple di-chromatic LED. Because we only used one type of QD suspension, the obtained color-rendering index was fairly low. For example, at $d = 0.8$ cm the LER = 349.1 lm/w and CRI = 28.0. To boost light efficiency and the color-rendering index, we could use multiple QD suspensions with emission spectra covering the entire visible range. As our simulation result indicates, we can greatly improve the light efficiency and color-rendering properties by using tri-chromatic or quad-chromatic LED.

Device lifetime is another important consideration for the proposed CT-tunable LED. It is mainly determined by the lifetime of the employed QD material. From [24], QD film has been demonstrated to have long-term stability with $>30,000$ operation

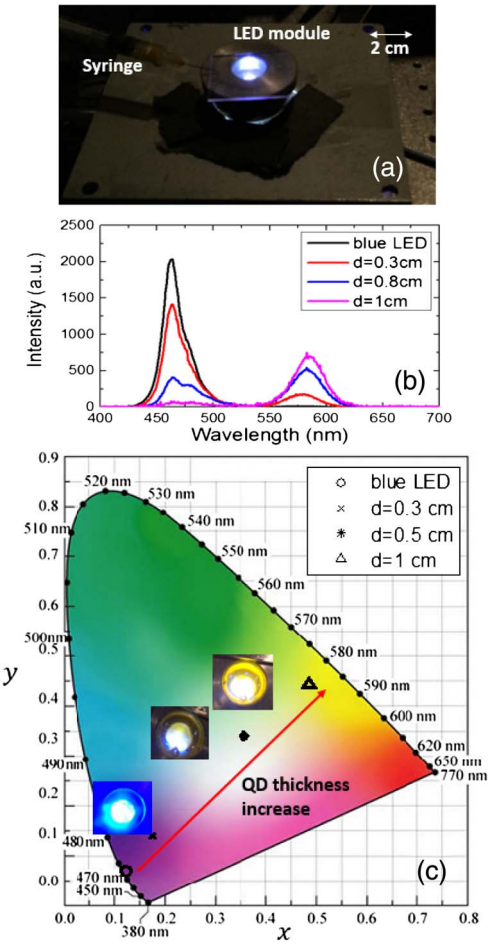

Fig. 6. (a) Photograph of the color-tuning LED setup. (b) Emission spectrum of color-tunable LED for different QD suspension thicknesses and (c) color coordinates of the color-tunable LED (the insets show the recorded color image of LED).

hours, and QD suspension can have a shelf life for almost one year. With the advancement of QD material (such as improvement in core-shell structure and organic ligands), our proposed LED is expected to have a sufficient long device lifetime.

The cost and size of the proposed device is mainly determined by the piston driving method. For the prove-of-concept experiment we implemented a step motor and syringe. To reduce the device cost and size we could activate the piston position by an electronically controlled screw or ferrofluids [21,22]. Such tuning methods have already been demonstrated in an adaptive lens for continuous focus tuning. The tuning step is mainly determined by the screw pitch or ferrofluid moving precision. A smaller tuning step is favored for fine tuning. With these mature and low-cost piston-driving methods, the LED size and cost could be reduced substantially.

5. Conclusion

We proposed a color-tunable LED consisting of a blue LED as light source and quantum dot suspension as a color-conversion medium. The LED color

temperature can be tuned by varying the liquid volume of each quantum dot suspension with different photoluminescence color. We simulated and optimized the light efficiency and color quality of the color-tunable LED and also prepared a prototype to prove the concept. Our proposed color-tunable LED provides an alternative approach for color tuning. Compared to existent multi-LED based systems, our proposed device may have shortcomings in cost and long-term stability. But these drawbacks can be overcome by the vast advancement of QD material quality and various piston tuning methods. Our proposed LED can potentially offer several advantages: excellent color-rendering property and high light efficiency, simple mechanical structure and driving mechanism, as well as high energy efficiency. It could be attractive to circadian rhythm regulation and healthy lighting.

References

1. E. F. Schubert, *Light-Emitting Diodes* (Cambridge, 2006).
2. E. F. Schubert and J. K. Kim, "Solid-state light sources getting smart," Science **308**, 1274–1278 (2005).
3. G. X. He and L. H. Zheng, "Color temperature tunable white-light light-emitting diode clusters with high color rendering index," Appl. Opt. **49**, 4670–4676 (2010).
4. C. Hoelen, J. Ansems, P. Deurenberg, W. van Duijneveldt, M. Peeters, G. Steenbruggen, T. Treurniet, A. Valster, and J. W. ter Weeme, "Color tunable LED spot lighting," Proc. SPIE **6337**, 63370Q (2006).
5. I. Speier and M. Salsbury, "Color temperature tunable white light LED system," Proc. SPIE **6337**, 63371F (2006).
6. M.-C. Chien and C.-H. Tien, "Multispectral mixing scheme for LED clusters with extended operational temperature window," Opt. Express **20**, A245–A254 (2012).
7. G. Dietrich and B. Karin, "Definition and measurement of circadian radiometric quantities," in *Proceedings of the International Commission on Illumination Symposium* (2004), pp. 129–132.
8. J. H. Oh, S. J. Yang, and Y. R. Do, "Healthy, natural, efficient and tunable lighting: four-package white LEDs for optimizing the circadian effect, color quality and vision performance," Light Sci. Appl. **3**, e141 (2014).
9. J. M. Spaulding, M. R. Thompson, and R. E. Levin, "Human preference in tunable solid state lighting," Proc. SPIE **7954**, 795403 (2011).
10. J. Lim, W. K. Bae, J. Kwak, S. Lee, C. Lee, and K. Char, "Perspective on synthesis, device structures, and printing processes for quantum dot displays," Opt. Mater. Express **2**, 594–628 (2012).
11. T. Erdem, S. Nizamoglu, X. W. Sun, and H. V. Demir, "A photometric investigation of ultra-efficient LEDs with high color rendering index and high luminous efficacy employing nanocrystal quantum dot luminophores," Opt. Express **18**, 340–347 (2010).
12. Z. Luo, Y. Chen, and S.-T. Wu, "Wide color gamut LCD with a quantum dot backlight," Opt. Express **21**, 26269–26284 (2013).
13. Y. Shirasaki, G. J. Supran, M. G. Bawendi, and V. Bulovic, "Emergence of colloidal quantum-dot light-emitting technologies," Nat. Photonics **7**, 13–23 (2012).
14. Z. Luo, D. Xu, and S.-T. Wu, "Emerging quantum-dots-enhanced LCDs," J. Disp. Technol. **10**, 526–539 (2014).
15. Z. Luo and S. T. Wu, "A spatiotemporal four-primary color LCD with quantum dots," J. Disp. Technol. **10**, 367–372 (2014).
16. Z. Luo, S. Xu, Y. Gao, Y. H. Lee, and S. T. Wu, "Quantum dots enhanced liquid displays," J. Disp. Technol. **10**, 987–990 (2014).
17. J. Y. Tsao, I. Brener, D. F. Kelley, and S. K. Lyo, "Quantum-dot-based solid-state lighting with electric-field-tunable chromaticity," J. Disp. Technol. **9**, 419–426 (2013).
18. S. A. Empedocles and M. G. Bawendi, "Quantum-confined stark effect in single CdSe nanocrystallite quantum dots," Science **278**, 2114–2117 (1997).
19. J. S. Kamal, R. Gomes, Z. Hens, M. Karvar, K. Neyts, S. Compernolle, and F. Vanhaecke, "Direct determination of absorption anisotropy in colloidal quantum rods," Phys. Rev. B **85**, 035126 (2012).
20. S. Xu, Y. Liu, H. Ren, and S.-T. Wu, "A novel adaptive mechanical-wetting lens for visible and near infrared imaging," Opt. Express **18**, 12430–12435 (2010).
21. S. Xu, H. Ren, and S.-T. Wu, "Adaptive liquid lens actuated by liquid crystal pistons," Opt. Express **20**, 28518–28523 (2012).
22. H. C. Cheng, S. Xu, Y. Liu, S. Levi, and S.-T. Wu, "Adaptive mechanical-wetting lens actuated by ferrofluids," Opt. Commun. **284**, 2118–2121 (2011).
23. W. Davis and Y. Ohno, "Color quality scale," Opt. Eng. **49**, 033602 (2010).
24. J. Chen, V. Hardev, and J. Yurek, "Quantum-dot displays: Giving LCDs a competitive edge through color," Inf. Disp. **29**, 12–17 (2013).